

EVALUATION OF EXTRA PIXEL INTERPOLATION WITH MASK PROCESSING FOR MEDICAL IMAGE SEGMENTATION WITH DEEP LEARNING

Olivier Rukundo

ABSTRACT

In this study, the author evaluated the use of an extra pixel interpolation algorithm with mask processing versus non-extra pixel interpolation algorithm when interpolating training dataset images and masks for medical image segmentation with deep learning. The author also examined scenarios of interpolating dataset images and masks using different algorithms: extra pixel for interpolating dataset images and non-extra pixel for interpolating dataset masks. The evaluation outcomes revealed that training on datasets consisting of images and masks both interpolated using the extra pixel's bicubic interpolation (BIC) resulted in better segmentation accuracy compared to using either the non-extra pixel's nearest neighbor interpolation (NN) or BIC for dataset images and NN for dataset masks. Specifically, the evaluation revealed that the BIC-BIC network was a 8.9578 % (with image size 256×256) and a 1.0496 % (with image size 384×384) increase of NN-NN network compared to the NN-BIC network which was a 8.3127 % (with image size 256×256) and a 0.2887 % (with image size 384×384) increase of NN-NN network.

Index Terms— Interpolation, Mask Processing, Image Segmentation, Deep Learning

1. INTRODUCTION

A novel interpolation mask processing method was introduced in [6] to remove extra class labels in interpolated masks. Unlike in [6], here, the author further evaluates the interpolation mask processing strategy, proposed in [6] using extra pixel category-based networks against the non-extra pixel category-based network and the dedicated combination of the two in medical image segmentation with deep learning. In deep learning, a class of deep neural networks commonly applied to visual imagery is the convolutional neural network (CNN) [6]. Here, the CNN architecture of interest is the U-net [5], due to its higher performance in medical image segmentation tasks [1], [2],[6]. It is worth noting that the non-extra pixel category algorithm, nearest neighbor, is routinely used to interpolate masks due to its inherent advantage of not creating non-original or extra class labels in the interpolated masks [6]. Despite that, in [6], the author demonstrated that the fact that, it produces heavy artefacts [7], [8], [9], reduces the quality of interpolated images thus negatively affecting the

accuracy of medical segmentation with deep learning. The rest of the paper includes part 2 which covers the material and method parts and part 3 which covers experimental results and relevant discussions.

2. MATERIALS AND METHODS

2.1. U-net architecture

U-Net is a CCN architecture widely used for semantic segmentation tasks [5]. It features a U-shaped design, comprising contracting and expansive paths. In our experiments, we used the U-Net Layers function in MATLAB to easily create a U-Net architecture for semantic segmentation. This function follows the U-shaped architecture described in the original U-Net paper [5].

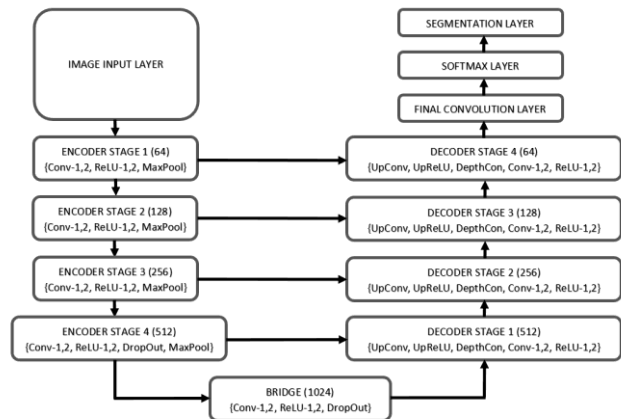


Figure 1: U-net architecture. *Conv* means convolution. *ReLU* is rectified linear unit. *DepthConv* is depth concatenation. *UpConv* means up-convolution or transposed convolution. *MaxPool* is Max Pooling, [6]

The contracting path consists of repeating blocks of convolution, ReLU activation, and max pooling. The expansive path involves transposed convolution, ReLU activation, concatenation with the downsampled feature map, and additional convolution. The U-Net Layers function provides options to customize the network, but note that it is just one implementation of the U-Net architecture. For more information, refer to the MATLAB documentation [4] and [3]. Figure 1 shows the input and output layers, as well as the intermediate layers and connections, of a deep learning

network as visualized by the *analyzeNetwork* function in MATLAB.

2.2. Interpolation mask processing

Interpolated mask processing or handling strategy was first proposed in [6] to remove extra class labels in interpolated GT images to keep the number of classes of output mask as input mask. The developed strategy uses three important techniques/operations, namely (1) thresholding, (2) median-filtering, and (3) subtraction to remove extra class in the five steps, as shown in [6]. Figure 2 illustrates where the interpolation mask processing strategy, proposed in [6], is used or applied to achieve the output mask with the number of classes as input mask.

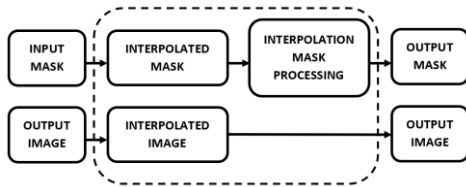


Figure 2: Illustration of the application of the interpolation mask processing strategy during the interpolation of training dataset images and masks.

3. RESULTS AND DISCUSSIONS

3.1. Training data

The reference dataset consisted of 1500 LGE MRI images and corresponding masks of the size 128×128 . This dataset is a part of the dataset used in [6]. Images and masks were upsampled to create new datasets. Each mask consisted of three classes, with class IDs, corresponding to 255-, 128-, and 0-pixel labels. As done in [1] and [2], each training dataset was split into three sets, namely: the training set (60% of the training dataset), the validation set (20% of the training dataset), and the test set (20% of the training dataset). Note that the execution environment was single-GPU with the Nvidia GeForce RTX 3070 graphic card and 11th Gen Intel(R) Core(TM) i7-11700F @ 2.50GHz, 2496 Mhz, 8 Core(s), 16 Logical Processor(s).

3.2. Hyperparameter settings

Here, the author referred to [1] and manually adjusted training hyperparameter values, with no new adjustments if 90% of training accuracy was reached during the first 10% of all epochs. Training hyperparameters that were not listed below remained set to default. The number of epochs = 60; the minimum batch size = 8; the initial learning rate = 0.0001; L2 regularization = 0.000005; optimizer = Adam (adaptive moment estimation algorithm).

3.3. Data augmentation

To augment both image and mask, the data augmentation options used included the random reflection in the left-right direction as well as the range of vertical and horizontal translations on the pixel interval ranging from -10 to 10.

3.4. Loss function

The loss function used was the default cross-entropy function provided by the U-Net Layers function. Further information on this function can be found in the MATLAB documentation [3].

3.5. Results

3.5.1. Regional networks performance



Figure 3: Networks trained with datasets consisting of 256×256 images and masks: NN-NN, NN-BIC, and BIC-BIC

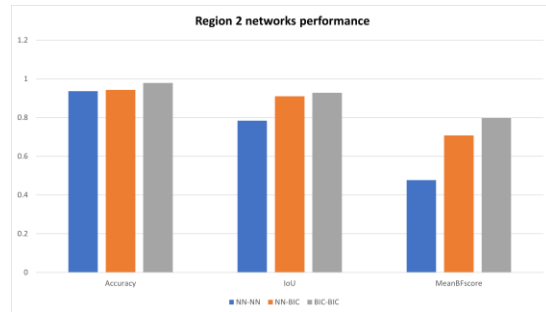


Figure 4: Networks trained with datasets consisting of 256×256 images and masks: NN-NN, NN-BIC, and BIC-BIC

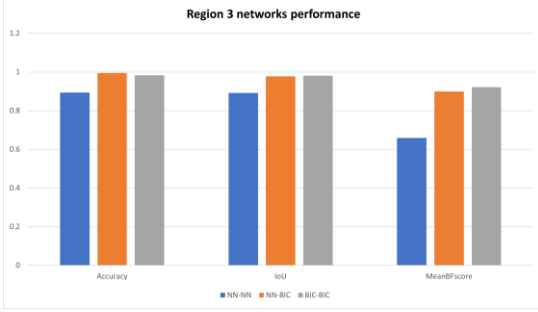


Figure 5: Networks trained with datasets consisting of 256×256 images and masks: NN-NN, NN-BIC, and BIC-BIC

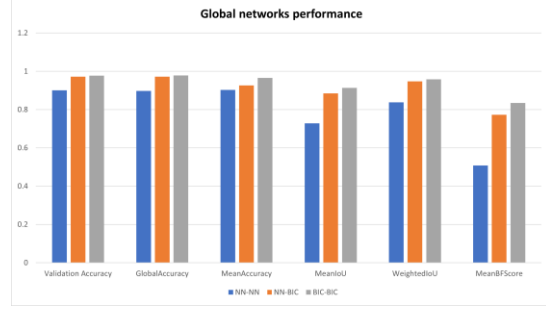


Figure 9: Global performance of networks trained with datasets consisting of 256×256 images and masks: NN-NN, NN-BIC, and BIC-BIC

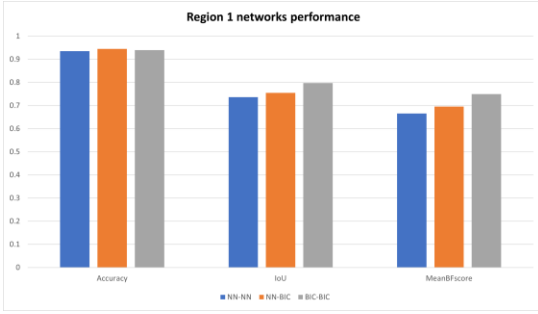


Figure 6: Networks trained with datasets consisting of 384×384 images and masks: NN-NN, NN-BIC, and BIC-BIC

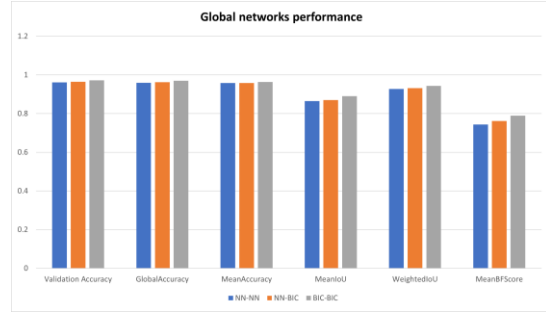


Figure 10: Global performance of networks trained with datasets consisting of 384×384 images and masks: NN-NN, NN-BIC, and BIC-BIC



Figure 7: Networks trained with datasets consisting of 384×384 images and masks: NN-NN, NN-BIC, and BIC-BIC

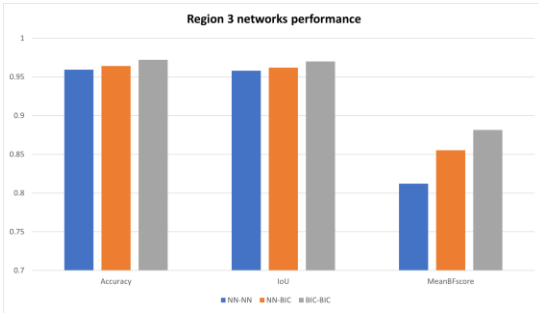


Figure 8: Networks trained with datasets consisting of 384×384 images and masks: NN-NN, NN-BIC, and BIC-BIC

3.6. Discussions

In this section, the percentage increase is used to provide a clear and concise representation of the progress made by extra pixel category interpolation-based networks (NN-BIC or BIC-BIC) compared to the initial values or scores achieved by the non-extra pixel category interpolation-based network (NN-NN). Equation 1's output means that extra pixel category interpolation-based network (A) is $x\%$ increase of non-extra pixel category interpolation-based network (B). Also, it means that the higher percentage increase towards 100%, the better score or the closer to the maximum score of 1.

$$\% \text{ increase} = \frac{(A - B)}{B} \times 100 \quad (1)$$

Table 1 and Table 2 show percentage increase rates in terms of Accuracy. Table 3 and Table 4 show percentage increase rates in terms of IoU. Table 5 and Table 6 show percentage increase rates in terms of meanBF. Table 7 shows percentage increase rates in terms of global accuracy. As can be seen, in Table 1, Table 2, Table 3, Table 4, Table 5, and Table 6, the BIC-BIC network achieved always a better average percentage increase than both NN-NN and NN-BIC networks.

3.5.2. Global networks performance

Table 1: Extra pixel category interpolation-based networks percentage increase of NN-NN - case: **Accuracy** | size: **256 × 256**

	Region 1	Region 2	Region 3
NN-BIC (2.5%)	-4.1334 %	0.6599 %	11.2193 %
BIC-BIC (7.0%)	6.6446 %	4.5382 %	9.9760%

Table 2: Extra pixel category interpolation-based networks percentage increase of NN-NN - case: **Accuracy** | size: **384 × 384**

	Region 1	Region 2	Region 3
NN-BIC (-0.03%)	1.0640 %	-1.6684 %	0.4930 %
BIC-BIC (0.49%)	0.4823 %	-0.3261 %	1.3415 %

Table 3: Extra pixel category interpolation-based networks percentage increase of NN-NN - case: **IoU** | size: **256 × 256**

	Region 1	Region 2	Region 3
NN-BIC (25.5%)	51.0539 %	16.0581 %	9.63173 %
BIC-BIC (30.5%)	63.4582 %	18.2819 %	9.9827 %

Table 4: Extra pixel category interpolation-based networks percentage increase of NN-NN - case: **IoU** | size: **384 × 384**

	Region 1	Region 2	Region 3
NN-BIC (0.7%)	2.5206 %	-0.5792 %	0.4185 %
BIC-BIC (3.3%)	8.3745 %	0.3680 %	1.2461 %

Table 5: Extra pixel category interpolation-based networks percentage increase of NN-NN - case: **meanBF** | size: **256 × 256**

	Region 1	Region 2	Region 3
NN-BIC (55.7%)	82.264 %	48.4785 %	36.515 %
BIC-BIC (69.5%)	101.5649 %	67.2667 %	39.8251 %

Table 6: Extra pixel category interpolation-based networks percentage increase of NN-NN - case: **meanBF** | size: **384 × 384**

	Region 1	Region 2	Region 3
NN-BIC (2.4%)	4.5472 %	-2.5469 %	5.3134 %
BIC-BIC (6.3%)	12.5871 %	-2.1037 %	8.5229 %

Table 7: Extra pixel category interpolation-based networks percentage increase of NN-NN - case: **Global accuracy**

	256 × 256 case	384 × 384 case
NN-BIC	8.3127 %	0.2887 %
BIC-BIC	8.9578 %	1.0496 %

It is worth noting that the global accuracy was of interest here, but referring to **Figure 12**, it was clear that the BIC-BIC network outperformed the NN-NN and NN-BIC networks in terms of other cases, such as Validation Accuracy, MeanAccuracy, MeanIoU, WeightedIoU, and MeanBFScore for both 256 x 256 and 384 x 384 cases, respectively, thus suppressing the need for adding additional relevant percentages increase tables, in this part.

4. CONCLUSION

The author's evaluation confirmed that using extra pixel category interpolation algorithm with interpolation mask processing strategy proposed in [6], generally, improved the

accuracy of medical image segmentation with deep learning. Specifically, interpolation mask processing method enabled the BIC algorithm to achieve better segmentation accuracy compared to using either NN algorithm for both dataset images and masks or BIC for dataset images and NN for dataset masks. Results also indicated a higher percentage increase with dataset cases of image size 256 x 256 than 384 x 384.

5. REFERENCES

- [1] Rukundo, O., Effect of the regularization hyperparameter on deep learning-based segmentation in LGE-MRI, Proc. SPIE 11897, Optoelectronic Imaging and Multimedia Technology VIII, 1189717, 2021
- [2] Rukundo, O., Evaluation of deep learning-based myocardial infarction quantification using segment CMR software, Proc. SPIE 11897, Optoelectronic Imaging and Multimedia Technology VIII, 1189716, 2021
- [3] Specify Layers of Convolutional Neural Network, Mathworks, <<https://se.mathworks.com/help/deeplearning/ug/layers-of-a-convolutional-neural-network.html>>, Accessed: 2023-02-12
- [4] 2-D convolutional layer, Mathworks, <<https://se.mathworks.com/help/deeplearning/ref/nnet.cnn.layer.convolution2dlayer.html>>, Accessed: 2023-02-12
- [5] Ronneberger, O., Fischer, P., Brox, T., U-Net: convolutional networks for biomedical image segmentation, In: Navab N., Hornegger J., Wells W., Frangi A. (eds), MICCAI 2015, Part II, LNCS 9351, 2015, pp. 234–241
- [6] Rukundo, O. Effects of Image Size on Deep Learning. *Electronics* 2023, 12, 985
- [7] Rukundo, O.; Schmidt, S. Stochastic Rounding for Image Interpolation and Scan Conversion. *Int. J. Adv. Comput. Sci. Appl.* 2022, 13, pp. 13–22
- [8] Rukundo, O., Non-extra pixel interpolation, *Int J Image Graph* 2020, 20, 2050031, pp.1-14
- [9] Rukundo, O., Schmidt, S.E., Von Ramm, O.T., Software implementation of optimized bicubic interpolated scan conversion in echocardiography, arXiv:2005.11269, 2020